Conformations of Methyl 2'-Deoxy-α-D-ribofuranoside and Methyl 2'-Deoxy-β-D-ribofuranoside. A Proton Magnetic Resonance Spectroscopy and Molecular Mechanics Study

J. Raap,*[1] J. H. van Boom,[1] H. C. van Lieshout,[2] and C. A. G. Haasnoot[2,3]

Contribution from the Gorlaeus Laboratories, State University of Leiden, P.O. Box 9502, 2300 RA Leiden, The Netherlands, and Laboratory of Biophysical Chemistry, University of Nijmegen, Toernooiveld, 6525 ED Nijmegen, The Netherlands. *Received March 16, 1987*

Abstract: The conformation of several 2'-deoxy-α-D-ribofuranoside and 2'-deoxy-β-D-ribofuranoside derivatives in solution were studied by ^{1}H NMR at 300 MHz, using vicinal coupling constants and chemical shifts obtained as a probe. The conformation of the five-membered sugar ring of these derivatives in solution is quantitatively described in terms of the concept of pseudorotation. It appeared that, in D_2O solution, methyl 2'-deoxy-β-D-ribofuranoside (**1b**) is engaged in an equilibrium between two conformational species. The geometry of the *N*-type conformer can be described as an intermediate between ^1_2T and $_2E$ (P = 335°, Φ_m = 45°), whereas that of the *S*-type conformer can be denoted as a ^4E conformation (P = 234°, Φ_m = 42°). It is shown that the conformation of the sugar ring of **1b** is quite different from the geometry of the *N*-type conformer usually observed for β-nucleosides(tides). This observation demonstrates the dominant influence of the substituent at $C_{1'}$ on the conformation of the five-membered ring. A comparison of the pseudorotational parameters of the *N*-type conformation of the *p*-nitrobenzoylated derivative of **1b** (**2b**) in solution with those observed in the solid state shows that the former ($P(N)$ = 340°, $\Phi_m(N)$ = 45°) differs significantly from the latter ($P(N)$ = 291.7°, $\Phi_m(N)$ = 33.7°). This discrepancy is attributed to crystal-packing forces in the solid-state structure. The conformational features of methyl 2'-deoxy-α-D-ribofuranoside (**1a**) (in D_2O solution) as deduced from ^{1}H NMR indicate that in this compound an *S*-type conformation of the five-membered sugar ring is strongly favored. The geometry of the latter conformation is best described as an $_1E$ form (P = 132°, Φ_m = 40°). Our analyses of ^{1}H NMR data are complemented by a molecular mechanics study of compounds **1a** and **1b**. It is shown that the geometric features of **1a** and **1b** are very well reproduced by MM-2 force field calculations. However, the calculated relative energies of the distinct conformers in these compounds are contradicted by the conformational populations determined experimentally by NMR. Notwithstanding, the application of Allinger's MM-2 provided a better insight into the experimental results. The results of the present study on the conformational properties of **1a** and **1b** can be interpreted in terms of the well-known gauche and anomeric effects: The *N*-type conformer of **1b** can be explained by an anomeric stabilization of the sugar ring, whereas, in contrast, the *S*-type conformer of **1b** is stabilized by the occurrence of a predominant gauche effect. Furthermore, it is suggested that, in the *S*-type conformer of compound **1a**, both the anomeric and the gauche effects are operative. The ^{1}H NMR spectra for **1a** and **1b** permitted an evaluation of the relative populations of the three conformers around the exocyclic $C_{4'}$–$C_{5'}$ bond. Our data indicate that for the *N*-type pucker the gauche$^+$ rotamer might be forbidden.

Double-helical complexes formed from so-called "base-deleted" oligonucleotides[4] form convenient models for the investigation of the recognition mechanism of apurinic or apyrimidinic (AP) sites[5] in nucleic acids by repairing proteins. The interaction between the protein and the AP site is likely to be influenced by the conformational features of the base-deleted sugar residue 2'-deoxy-D-ribofuranose.[6] Therefore, the study of the solution conformations of this sugar residue will bring about basic knowledge necessary for understanding the complex behavior of the specific binding of the AP site to the enzyme AP-endonuclease.

By application of ^{1}H NMR techniques to the base-deleted sugar, the preferred solution conformations can be derived.[7,8] However, the NMR investigation of an aqueous solution of 2'-deoxy-D-ribofuranose is hampered by the fact that the hemiacetal function of the sugar is configurationally unstable. This difficulty, originating from mutarotation in water, complicates a detailed conformational analysis. In recent studies of base-deleted D oligonucleotides, the problem has been circumvented by designing sugar analogues that are stable in aqueous solution: 1',2'-dideoxy-D-ribofuranose[4] and 1'-(2'-deoxy-β-D-ribofuranosyl) cyanide.[9] Our approach to solving this problem is to prevent the mutarotation of the anomeric site by methylation of the $O_{1'}$ position.

It is the aim of this study to examine the conformational properties of methyl 2'-deoxy-α-D-ribofuranoside (**1a**) and methyl 2'-deoxy-β-D-ribofuranoside (**1b**) in aqueous solution (Figure 1). Until now little was known about the conformational features of these compounds: To the best of our knowledge, the conformation of **1a** has as yet not been reported, whereas the conformational behavior of the five-membered ring of **1b** has been described in qualitative terms only by Gerlt and Youngblood.[10] The latter authors concluded from a qualitative analysis of the NMR vicinal coupling constants that the sugar ring preferentially populates the 3'-endo (^3E) type of pucker. However, they were not able to analyze their ^{1}H NMR spectra in a consistent manner (vide infra). Moreover, some doubts about the experimental analysis by Gerlt and Youngblood have been expressed.[11]

Recently, the solid-state structure of methyl 2'-deoxy-3',5'-O-bis(*p*-nitrobenzoyl)-β-D-ribofuranoside (**2b**; see Figure 1) has been investigated in our laboratories by means of X-ray crystallography.[12] The puckering and conformation of the 2'-deoxyribofuranose ring were quantitatively described by the concept of pseudorotation.[7,13,14] It appeared that in the solid state the sugar adopts a twist conformation, which can be denoted as ^1_0T (P = 291.7°, Φ_m = 33.7°).

(1) Department of Organic Chemistry, State University of Leiden.
(2) Laboratory of Biophysical Chemistry, University of Nijmegen.
(3) Present address: Unilever Research Laboratory, Olivier van Noortlaan 120, 3133 AT Vlaardingen, The Netherlands.
(4) Millican, T. A.; Mock, G. A.; Channcey, M. A.; Patel, T. P.; Eaton, M. A. W.; Gunning, J.; Cutbush, S. D.; Neidle, S.; Mann, J. *Nucleic Acids Res.* **1984**, *12*, 7435.
(5) For a review, see: Lindahl, T. *Annu. Rev. Biochem.* **1982**, *51*, 61.
(6) The nomenclature is not strictly according to IUPAC conventions for carbohydrates but rather adheres to the latest IUPAC–IUB nucleoside recommendations because the fragments under study will be compared with nucleoside sugars.
(7) Altona, C.; Sundaralingam, M. *J. Am. Chem. Soc.* **1973**, *95*, 2333.
(8) Haasnoot, C. A. G.; de Leeuw, F. A. A. M.; De Leeuw, H. P. M.; Altona, C. *Org. Magn. Reson.* **1981**, *15*, 43.
(9) Pochet, S.; Huynh-Dinh, T.; Neumann, J.-M.; Tran-Dinh, S.; Adam, S.; Taboury, J.; Taillandier, E.; Igolen, J. *Nucleic Acids Res.* **1986**, *14*, 1107.
(10) Gerlt, J. A.; Youngblood, A. V. *J. Am. Chem. Soc.* **1980**, *102*, 7433.
(11) Wiórkiewicz-Kuczera, J.; Rabczenko, A. *J. Chem. Soc., Perkin Trans 2* **1986**, 437.
(12) Raap, J.; Bruins Slot, H. J.; Beurkens, P. T.; van Wietmarschen, J. A. C.; Smits, J. J. M.; Haasnoot, C. A. G. *Acta Crystallogr., Sect. B: Struct. Sci.* **1987**, *B43*, 219.
(13) Altona, C.; Geise, H. J.; Romers, C. *Tetrahedron* **1968**, *24*, 13.
(14) Altona, C.; Sundaralingam, M. *J. Am. Chem. Soc.* **1972**, *94*, 8205.

0002-7863/88/1510-2736$01.50/0

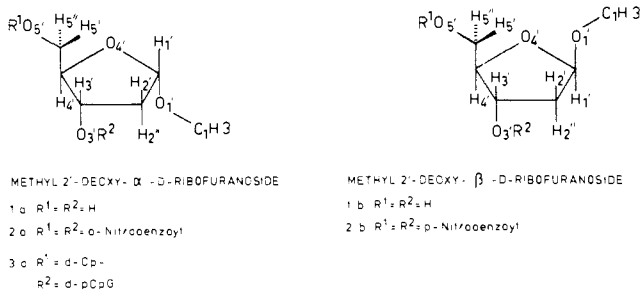

Figure 1. Structure of the studied analogues of the base-deleted sugar 2'-deoxy-D-ribofuranose: methyl 2'-deoxy-α-D-ribofuranoside (**1a**), methyl 2'-deoxy-β-D-ribofuranoside (**1b**), their *p*-nitrobenzoylated derivatives (**2a**, **2b**), and the α-anomeric sugar (**3a**) incorporated in the tetrameric D oligonucleotide d(CpSpCpG), where S stands for methyl 2'-deoxy-α-D-ribofuranoside(yl).

It has often been a matter of debate whether or not conformational data based on studies of the crystalline state of a compound are transferable to the solute state. The conformation that is favored in the crystal need not be a priori the (predominant) one in solution; in fact, in particular cases it has been shown that the crystal structure does not occur in solution at all.[15]

It is for these reasons that a conformational analysis of the title compounds in solution was deemed necessary. To this end, the present paper reports the results of a combined proton magnetic resonance and molecular mechanics study of methyl 2'-deoxy-α-D-ribofuranoside and methyl 2'-deoxy-β-D-ribofuranoside.

Methods

There are three conformational degrees of freedom available to ribofuranosides that can be monitored by ^{1}H NMR: i.e. two related to the sugar ring (the pseudorotational phase angle P and the puckering amplitude Φ_m[14]) and one concerning the $C_{4'}$–$C_{5'}$ side chain [the torsion angle γ ($O_{5''}$-$C_{5'}$-$C_{4'}$-$C_{3'}$)]. The proton–proton torsion angles in a β-D-ribofuranoside ring are related to the pseudorotational parameters of the sugar moiety according to eq 1a–e (taken from ref 8). Since the so-called "generalized

$$\phi_{1'2'} = 121.4 + 1.03\Phi_m \cos (P - 144) \quad (1a)$$

$$\phi_{1'2''} = 0.9 + 1.02\Phi_m \cos (P - 144) \quad (1b)$$

$$\phi_{2'3'} = 2.4 + 1.06\Phi_m \cos P \quad (1c)$$

$$\phi_{2''3'} = 122.9 + 1.06\Phi_m \cos P \quad (1d)$$

$$\phi_{3'4'} = -124.0 + 1.09\Phi_m \cos (P + 144) \quad (1e)$$

Karplus equation"[16] links the torsion angles Φ_{HH} in eq 1a–e to the corresponding proton–proton coupling constants, it is, at least in principle, possible to determine the sugar conformation (P and Φ_m) from the experimental vicinal coupling constants.[8,17]

The pseudorotational parameters of the α-anomers may be determined from eq 2a–e. These equations were derived on the

$$\phi_{1'2'} = -1.6 + 0.97\Phi_m \cos (P - 144.1) \quad (2a)$$

$$\phi_{1'2''} = -122.1 + 1.00\Phi_m \cos (P - 145.5) \quad (2b)$$

$$\phi_{2'3'} = 1.5 + 1.04\Phi_m \cos (P + 0.5) \quad (2c)$$

$$\phi_{2''3'} = 122.0 + 1.04\Phi_m \cos (P - 0.4) \quad (2d)$$

$$\phi_{3'4'} = -124.6 + 1.03\Phi_m \cos (P + 142.6) \quad (2e)$$

basis of the "extended pseudorotational equations"[18] in conjunction with a correlation between the proton–proton torsion angles and the endocyclic torsion angles derived from a series of structures calculated for compound **1a** using Allinger's MM-2 program.[19]

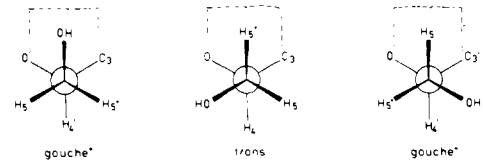

Figure 2. Three "classical" conformations of the exocyclic CH_2OH group about the $C_{4'}$–$C_{5'}$ bond.

It is noted that the empirical parameters of the pseudorotational eq 2a–e are in reasonable agreement with those estimated earlier for α-nucleosides.[8]

From ^{1}H NMR studies of nucleoside derivatives, it is well established[7,8] that the "flexible" 2'-deoxyribofuranose ring may occur in a fast equilibrium (relative to the ^{1}H NMR time scale) between two conformations.[7,8,14] Two classes of conformers can be distinguished: the *N*-type (phase angle of pseudorotation $-90° < P(N) < +90°$) and the *S*-type ($90° < P(S) < 270°$).[14] When eq 1a–e or 2a–e are applied and time averaging of the J couplings is accounted for, the conformational parameters $P(N)$, $\Phi_m(N)$, $P(S)$, and $\Phi_m(S)$ and the respective conformational populations X_N and X_S can be deduced from the five vicinal proton–proton couplings with a least-squares minimization procedure developed by Haasnoot et al.[8]

The conformation of the exocyclic moiety $C_{4'}$–$C_{5'}$ may be determined by an analysis of the vicinal coupling constants $^3J_{4'5'}$ and $^3J_{4'5''}$. These coupling constants can be interpreted in terms of g^+, t, and g^- rotamer populations (cf. Figure 2). The rapid interconversion between the three conformers yields weighted time-averaged NMR couplings, which are related to the coupling constants $^3J'$ and $^3J''$ of the individual conformers and their corresponding populations X_{g^+}, X_t, and X_{g^-} (in molar fractions; eq 3). The coupling constants $^3J'$ and $^3J''$ for the respective proton

$$^3J_{4'5'}\text{ (exptl)} = X_{g^+}{}^3J'_{g^+} + X_t{}^3J'_t + X_{g^-}{}^3J'_{g^-} \quad (3a)$$

$$^3J_{4'5''}\text{ (exptl)} = X_{g^+}{}^3J''_{g^+} + X_t{}^3J''_t + X_{g^-}{}^3J''_{g^-} \quad (3b)$$

torsion angles $\phi_{4'5'}$ and $\phi_{4'5''}$ of the individual rotamers can be calculated by means of the generalized Karplus equation[16] with the appropriate ϕ_{HH} torsion angles. These ϕ_{HH} angles can be translated into the backbone torsion angles ($O_{5'}$–$C_{5'}$–$C_{4'}$–$C_{3'}$) γ^+, γ^t, and γ^-. For **1a** and **1b**, the MM-2 energy-minimized structures show that the calculated torsion angle γ^- deviates from the "standard" γ^- value of −70°[20] depending slightly on the conformation of the sugar conformation; e.g., for **1b** the *N*- and *S*-type sugar ring conformations correspond to γ^- values of −56° and −70°, respectively. This observation leads us to propose that, instead of the standard $^3J'_{g^-}$ and $^3J''_{g^-}$ coupling constants,[20] the average coupling constants $^3J'_{g^-,av}$ and $^3J''_{g^-,av}$ (see eq 4a and b)

$$^3J'_{g^-,av} = X_N{}^3J'_{g^-,N} + (1 - X_N)^3J'_{g^-,S} \quad (4a)$$

$$^3J''_{g^-,av} = X_N{}^3J''_{g^-,N} + (1 - X_N)^3J''_{g^-,S} \quad (4b)$$

must be used in eq 3a and b. The average coupling constants are then related to both the conformational equilibrium of the sugar ring and the coupling constants of the g^- rotamer in the *N*- and *S*-type sugar conformation. The latter coupling constants were calculated by means of the generalized Karplus equation with the ϕ_{HH} torsion angles, which correspond to γ_N (=−56°) and γ_S (=−70°), respectively, together with the N/S populations determined in the conformational analysis of the sugar ring. In this way the γ populations X_{g^+}, X_t, and X_{g^-} given in e.g. Table III for **1a**, **2a**, **3a**, **1b**, and **2b** were calculated.

Results

Conformational Analysis of 1b and 2b Using ^{1}H NMR Vicinal Coupling Constants. Following well-established procedures,[8,15,28] pseudorotational analyses were carried out for **1b** (D_2O, 292 K)

(15) Haasnoot, C. A. G.; Lisskamp, R. M. J.; van Dael, P. A. W.; Noordik, J. H.; Ottenheijm, H. C. J. *J. Am. Chem. Soc.* **1983**, *105*, 5406–5414.
(16) Haasnoot, C. A. G.; De Leeuw, F. A. A. M.; Altona, C. *Tetrahedron* **1980**, *36*, 2783.
(17) de Leeuw, H. P. M.; Haasnoot, C. A. G.; Altona, C. *Isr. J. Chem.* **1980**, *20*, 108.
(18) de Leeuw, F. A. A. M.; van Kampen, P. N.; Altona, C.; Díez, E.; Esteban, A. L. *J. Mol. Struct.* **1984**, *125*, 67.
(19) Allinger, N. L. *J. Am. Chem. Soc.* **1977**, *99*, 8127. Allinger, N. L.; Yuh, Y. *QCPE* **1980**, *12*, 395.
(20) Haasnoot, C. A. G.; de Leeuw, F. A. A. M.; de Leeuw, H. P. M.; Altona, C.; *Recl. Trav. Chim. Pays-Bas* **1979**, *98*, 576.

Table I. Analysis of the Vicinal Coupling Constant Data (Hz) of **1b** and **2b**, Calculated Pseudorotational Parameters, and Mole Fractions

	1b							**2b**: $CDCl_3$; 292 K		
	D_2O; 271–346 K				$CDCl_3$; 292 K					
coupling	J_{exptl}[a]	J_{calcd}(I)[b]	J_{calcd}(II)[c]	J_{calcd}(II′)[d]	J_{exptl}	J_{calcd}(III)[c,e]	J_{calcd}(III′)[d,e]	J_{exptl}	J_{calcd}(III)[c,e]	J_{calcd}(III′)[d,e]
1′2′	2.7	1.3	3.1	3.1	2.0	2.4	2.4	2.0	2.5	2.6
1′2″	5.5	6.0	6.2	5.5	5.7	6.3	5.6	5.7	6.7	5.8
2′3′	6.7	9.0	6.8	6.8	6.8	7.5	7.5	7.4	7.2	7.2
2″3′	5.9	7.4	6.5	6.5	5.8	6.3	6.1	5.1	5.6	5.3
3′4′	4.2	3.5	4.0	3.9	3.8	3.6	3.5	3.0	3.2	3.0
rms		1.4	0.5	0.3		0.5	0.4		0.6	0.3
parameter		I	II	II′		III	III′		III	III′
X_N		1.00	0.61	0.52		0.58	0.47		0.49	0.37
$P(N)$		304	324	335		323	340		323	340
$\Phi_m(N)$		38	45	45		45	45		45	45
$P(S)$			225	234		243	249		243	249
$\Phi_m(S)$			42	42		41	41		41	41

[a] Average of three values determined from spectra recorded at 271, 292, and 346 K. Coupling constants are independent of temperature, within experimental error. [b] Vicinal coupling constants calculated for a one-state model. [c] Time-averaged values calculated for a two-state model. [d] Time-averaged values calculated for a two-state model, including a so-called Barfield correction.[21] [e] The coupling constant data observed for **1b** and **2b** in $CDCl_2$ were fitted while retaining the geometrical parameters constant and using the conformational population as the only variable to be optimized.

with the experimentally determined coupling constant data listed in Table I (see the Experimental Section).

In a first attempt, the analysis was carried out assuming that the sugar ring adopts a unique, single conformation. However, the observed couplings cannot be rationalized in terms of a single conformation for the five-membered ring as is shown by the large differences between the observed and calculated coupling constants (up to 2.3 Hz) for the ultimate "best" single conformer (compare column J_{exptl} with column J_{calcd}(I) in Table I).

Next, the possibility of a conformational equilibrium was considered. Assuming a rapid interconversion between two conformations of the five-membered sugar ring, the (time-average weighted) coupling constants are best accounted for by an approximately 6:4 conformational mixture of *N*- and *S*-type forms. Table I, column II, shows that the calculated vicinal coupling constants reproduce the couplings observed in the ^1H NMR spectrum rather well: the root mean square (rms) deviation between the observed and calculated couplings amounts to 0.5 Hz. Although the estimated error in the observed coupling constants is small (esd's <0.2 Hz) with respect to this rms value of 0.5 Hz, the latter value is in reasonable correspondence with the error, which one can expect on basis of the applied method of analysis (0.4 Hz).[16] However, scrutiny of the individual couplings in Table I reveals that $J_{1'2''}$ and $J_{2''3'}$ in particular are responsible for the rms deviation of 0.5 Hz. At this point we note that the pseudorotational parameters obtained from the observed couplings (Table I, column II) shows that the *N*- and *S*-type conformers can be characterized by a twist conformation ($P(N)$ = 324°, $\Phi_m(N)$ = 45°) and a distorted envelope conformation ($P(S)$ = 225°, $\Phi_m(S)$ = 42°), respectively. In the latter conformation $C_{4'}$ is located at the tip of the envelope, opposite to the $C_{1'}$–$C_{2'}$ fragment, which bears two cisoidal protons: $H_{1'}$ and $H_{2''}$. Semiempirical MO calculations have indicated that in the envelope geometry of tetrahydrofuran[21] the through-space interactions between the carbon–hydrogen orbitals of a C–C fragment and the orbitals about the carbon or oxygen, which resides at or near the tip of an envelope conformation, tend to reduced the cisoidal coupling between a pair of protons located opposite to the flap of the envelope. It was shown that this so-called "Barfield through-space transmission effect" can be approximated by a single $\cos^2$ function[22] (eq 5) where Δ^3J is the decrease in the cisoidal

$$\Delta^3J = T\cos^2(P - P_b) \quad (5)$$

coupling constant due to the transmission effect and P_b is the phase angle of pseudorotation of the envelope form for which a maximum is reached; for **1b** a maximum effect on $^3J_{1'2''}$ is expected for a value of P_b = 234° (^4E). The amplitude T strongly depends on the nature of the atom residing in the flap of the envelope via which orbitals the effect is realized. T is estimated to be of the order of ca. 0.5 Hz for oxygen and ca. 2 Hz for carbon;[22] the latter value was recently corroborated experimentally.[23] It follows that, in the case of the β-anomeric sugar **1b**, the Barfield transmission term is expected to be relatively large for $^3J_{1'2''}$ but rather small for the second cisoidal coupling $^3J_{2'3'}$. Since this Barfield effect is not accounted for by the generalized Karplus relation, it follows that the $^3J_{1'2''}$ coupling cannot be reproduced correctly in the current pseudorotational analysis: in other words, without a Barfield correction, the calculated time-average weighted $^3J_{1'2''}$ coupling will be overestimated.

When the above correction term (eq 5) is introduced in the least-squares fitting procedure, the calculated value of particularly $^3J_{1'2''}$ of each conformer is reduced and the overall rms deviation of the pseudorotational analysis drops from about 0.5 Hz (uncorrected) to about 0.3 Hz (corrected), column II′ of Table I. It is seen that the incorporation of a Barfield correction only slightly affects the outcome of the pseudorotational analysis: the conformational parameters found ($P(N)$ = 335°, $\Phi_m(N)$ = 45°, $P(S)$ = 234°, $\Phi_m(S)$ = 42°; X_N = 0.52) are close to those calculated earlier (see Table I, column II). In itself this finding is confidence inspiring as these calculations show that a single outlying observable ($^3J_{1'2''}$ in the former case) does not influence the results of the pseudorotational analysis to a great extent.

After determining the pseudorotational parameters and molar fractions of the *N*- and *S*-type conformers of **1b** in D_2O, we first fitted the coupling constant data observed for **1b** and **2b** in $CDCl_3$ (Table I) onto a two-state model while retaining the geometrical parameters found in D_2O and using the conformational populations as the only variable to be optimized. However, a significantly improved fit was found when the pseudorotational parameters describing the conformational equilibrium were also allowed to vary, dependent on solvent condition (cf. columns II′ (D_2O) and III′ ($CDCl_3$)). In other words, it appears that the pseudorotational phase angle of the *N*- and *S*-type sugar rings in D_2O differs slightly from the phase angle of the corresponding conformers occurring in $CDCl_3$ solution (Table I, column III′). The equilibrium constant of the *N*/*S* conformational equilibrium **1b** appears to be independent of change of temperature (within the range of 271–346 K) and alters only marginally upon change of solvent (D_2O, X_N

(21) Jaworski, A.; Ekiel, I.; Shugar, D. *J. Am. Chem. Soc.* **1978**, *100*, 4357.

(22) de Leeuw, F. A. A. M.; van Beuzekom, A. A.; Altona, C. *J. Comput. Chem.* **1983**, *4*, 428.

(23) Sedee, A. G. J.; Beljersbergen van Henegouwen, G. M. J.; Gulit, W.; Haasnoot, C. A. G. *J. Org. Chem.* **1985**, *50*, 4182.

(24) Altona, C.; Buijs, H. R.; Havinga, E. *Recl. Trav. Chim. Pays-Bas* **1966**, *85*, 973.

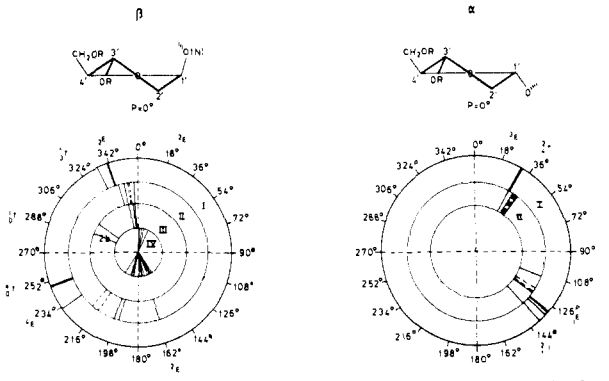

Figure 3. Pseudorotation wheels representing the phase angle (P) of the sugar ring conformations in glycofuranoside and nucleic acid constituents: (βI) P distribution of **1b** and **2b** in D_2O (or $CDCl_3$) solution. (βII) P distribution of **1b** as calculated by means of Allinger's MM-2. The P angles of energy-minimized structures are indicated for all combinations of sugar puckers (N/S) and γ rotamers ($g^+/t/g^-$). In order to simulate the electrostatic shielding effects of the solvent, energy minimizations were carried out at different values of the dielectric constant: $\epsilon = 1.5$ (solid lines) and $\epsilon = 4.0$–12.0 (dashed lines). (βIII) P angle of the crystal structure of **2b** and the P distribution of four solid-state structures of β-glycofuranosides. (βIV) P distribution of 30 crystal structures of 2'-deoxynucleosides (**17**). (αI) P distribution of **1a**, **2a**, and **3a** in D_2O (or $CDCl_3$) solution. (αII) P distribution of **1a** as calculated by means of Allinger's MM-2 (cf. legend of βII).

= 0.52; $CDCl_3$, $X_N = 0.47$). As can be gleaned from the data listed in Table I for **2b**, *p*-nitrobenzoylation does not change the conformation of the sugar ring; it only affects the equilibrium constant: the N-type conformer of **2b** is somewhat less populated ($X_N = 0.37$) in comparison with that of **1b** in $CDCl_3$.

A comparison of the pseudorotational parameters of the N-type conformer of **2b** in solution with those observed in the solid state[12] shows that the former ($P(N) = 340°$, $\Phi_m(N) = 45°$) differs significantly from the latter ($P = 291.7°$, $\Phi_m = 33.7°$). This discrepancy induced us to call upon a third, independent method of investigating the conformational behavior of **1b** (vide infra).

Conformational Study of 1b by Means of Molecular Mechanics (MM-2). Force field calculations were performed for **1b** by Allinger's MM-2 program.[19] Steric energy was calculated as a function of the sugar pucker; however, parameters defining the conformation of the exocyclic groups (i.e. the exocyclic torsion angles: γ, O_5'–C_5'–C_4'–C_3'; χ', O_4'–C_1'–O_1'–C_1) were also taken into consideration.

Pilot calculations showed that the steric energy of **1b** increases by at least 13 kJ/mol upon changing the χ' value from 300° to 60° or 180°. On these grounds, structures with gauche$^+$ and trans conformations about the C_1'–O_1' bond are deemed to be high-energy conformations and were left out of further consideration. Hence, the conformational problem was restricted to determining the steric energy of **1b** as a function of P, Φ_m, and γ.

Following standard procedures, six local minima were determined for all combinations of sugar puckers (N/S) and γ rotamers ($g^+/t/g^-$). The puckering amplitudes of these minimum-energy sugar conformations, $\Phi_m(N) = 40°$ and $\Phi_m(S) = 37°$, are found to be independent of the conformation of the exocyclic C_5'–OH group. The pseudorotational phase angles of **1b**, calculated from the minimized structures, do depend on the orientation about γ and are given in Figure 3 (track βII). It is seen that the P values of the minimum-energy N-type sugars are concentrated within a relatively narrow region; $P(N) = 344$–$357°$. Comparison of the MM-2 structures with the N-type solution conformers as determined by NMR (Table I; Figure 3, track βI) reveals a good correspondence. The P values of the S-type conformers calculated by MM-2 fall within a range of $P(S) = 160$–$200°$. In this case the MM-2 structures deviate noticeably from the S-type genus of the solution conformers ($P(S) = 234$–$249°$). However, when the effective dielectric constant used in the MM-2 calculations was increased (from 1.5 to 4 or 12) in order to mimic the electrostatic shielding effects of the solvent, the MM-2 minimizations yielded the pseudorotational parameters $P(N) \sim 355°$, $\Phi_m \sim 38°$, $P(S) \sim 220°$, and $\Phi_m \sim 38°$. These P values of N- and S-type conformations are close to those of the solution conformers.

Further inspection of Figure 3 reveals that the range of P values of the S-type sugar pucker, obtained from either ^1H NMR or MM-2, is larger than that of the N-type pucker. We note that a similar observation has been made previously from the solid-state data of 2'-deoxynucleoside derivatives:[17] In that case the $P(N)$ values occur in the region $P(N) = 0$–$26°$, whereas $P(S)$ emcompasses the broader range of 145–214° (see also track IV in Figure 3). This wider range for $P(S)$ was considered[14,17] to be indicative for a greater pseudorotational freedom (pseudolibration; cf. ref 24) of the sugar ring in 2'-deoxynucleoside derivatives. The MM-2 calculations suggest that this property is retained in the 2'-deoxyribofuranoside **1b**. Taken together, our results show that in the case of **1b** the outcome of ^1H NMR and MM-2 are mutually consistent *as far as the geometry of the stable minima is concerned.*

Contrastingly, the relative energy contents of the distinct conformations calculated for **1b** disagree with those inferred from our NMR analysis (vide supra). From the MM-2 results it appears that the S-type ring conformations have relative energy contents ~4 kJ/mol higher than the most favored N-type conformation. However, the lack of a significant temperature dependence for the coupling constants of **1b** indicates that the enthalpy difference $\Delta H°$ is close to zero.[7] This finding entails a warning against drawing conclusions from differences between values of steric energy being in the order of 4 kJ/mol.

A comparison between tracks βI and βIII of Figure 3 shows that the phase angle of **2b** ($P = 291.7°$) determined from the crystal structure[12] occupies a position approximately halfway between the phase angles of the N- and S-type solution conformers ($P(N) = 340°$ and $P(S) = 249°$). Hence, the phase angle of the solid-state structure is centered in a region of the conformational wheel representation, which is normally associated with a presumed energy barrier separating the N- and S-type solution conformers involved in the thermal equilibrium. This view, originating from recent results of potential energy calculations of dG and dC,[25] was based on the finding that the energy varies in the order of 31.4 kJ/mol for dG (83.6 kJ/mol for dC) on pseudorotation from N to S via the 270° pathway (see also ref 26). Furthermore, it was suggested that the interconversion between the N- and S-type puckers preferentially follows a pathway via the lower barrier at $P = 90°$ (12.1 kJ/mol for both dG and dC). Apart from absolute values of energy, this picture agrees well with our calculations (MM-2) in the N- and S-type conformers of **1b** are separated by a relatively high energy barrier at $P = 270°$ (16.7 kJ/mol) and a relative low barrier at $P = 90°$ (7.5 kJ/mol); the energy values in parentheses are given relative to the minimum potential energy at $P = 350°$.

In other words, it seems that in the crystal structure the steric energy of **2b** is higher with respect to that of the individual solution conformations. Taking into account that three out of four remaining solid-state conformations reported in the literature for β-furanosides (cf. track βIII) do agree with the N-type conformations determined by NMR and MM-2, it is plausible to hold intermolecular crystal-packing forces responsible for the observed high-energy conformation of the sugar ring of **2b** in the solid state.

In summary, according to a large body of X-ray crystallographic data,[17] phase angles of pseudorotation of the five-membered sugar ring in 2'-deoxynucleoside derivatives occur in two distinct ranges (see Figure 3, track βIV). In contrast, Figure 3 shows that the P values for glycofuranosides in the solid state (track βIII) as well as in solution (Figure 3, tracks βI and βII) fall outside this range observed for 2'-deoxynucleoside constituents. In other words, the intrinsic conformational properties of 2'-deoxy-β-ribofuranosides differ substantially from the analogous 2'-deoxy-β-nucleosides. This is an important conclusion with respect to conformational studies of so-called base-deleted oligonucleotides, in which the

(25) Pearlman, D. A.; Kim, S.-H. *J. Biomol. Struct. Dyn.* **1985**, *3*, 99.
(26) Olson, W. K. *J. Am. Chem. Soc.* **1982**, *104*, 278.

Table II. Analysis of the Vicinal Coupling Constant Data (Hz) of **1a**, **2a**, and **3a**, Calculated Pseudorotational Parameters, and Mole Fractions

	1a								**2a**: $CDCl_3$; 292 K		**3a**: D_2O; 300 K	
	D_2O; 271 K		D_2O; 292 K		D_2O; 346 K		$CDCl_3$; 292 K					
coupling	J_{exptl}	$J_{calcd}(I)^{a,b}$	J_{exptl}	$J_{calcd}(I)^{a,b}$	J_{exptl}	$J_{calcd}(I)^{a,b}$	J_{exptl}	$J_{calcd}(II)^{a,c}$	J_{exptl}	$J_{calcd}(II)^{a,c}$	J_{exptl}	$J_{calcd}(III)^{a}$
1′2′	5.3	5.6	5.4	5.7	5.4	5.9	5.0	5.6	5.0	5.7	5.4	5.9
1′2″	1.0	1.7	1.3	1.9	1.7	2.3	0.9	1.4	0.4	1.7	1.0	1.4
2′3′	7.3	6.9	7.5	7.0	7.5	7.1	7.2	7.0	8.1	7.1	6.9	6.6
2″3′	2.3	1.6	2.5	1.9	3.1	2.5	2.2	1.2	2.2	1.6	1.5	1.2
3′4′	3.4	3.9	3.6	4.0	3.9	4.4	2.7	3.8	3.8	4.0	2.8	3.1
rms		0.5		0.5		0.5		0.7		0.9		0.4
parameter		I		I		I		II		II		III
$P(N)$		29		29		29		29		29		
$\Phi_m(N)$		26		26		26		32		32		
$P(S)$		132		132		132		130		130		136
$\Phi_m(S)$		40		40		40		40		40		39
X_S		0.94		0.87		0.79		0.99		0.95		1.00

[a] Vicinal coupling constants calculated for a two-state model, including a so-called Barfield correction.[21] [b] The coupling constant data observed for **1a** in D_2O at different temperatures were fitted while retaining the geometrical parameters constant and using the conformational population as the only variable to be optimized. [c] As note *b* but for **1a** and **2a** in $CDCl_2$.

(monomeric) AP site is in fact a 2′-deoxy-β-D-ribofuranose.

Conformational Analyses of 1a, 2a, and 3a. The second part of our investigation was dedicated to compounds **1a**, **2a**, and **3a** (Figure 1) containing an α-anomeric five-membered sugar ring. When a similar procedure as described for **1b** is followed, the results of pseudorotational analysis of **1a** in D_2O show (see Table II) that the conformational features of the 2′-deoxy-α-D-ribofuranoside ring, even at 271 K, are best (characterized by a rms value of 0.5 Hz) described in terms of a conformational equilibrium between *N*- and *S*-type conformers. The following pseudorotational parameters were obtained from the analyses: $P(N) = 29°$, $\Phi_m(N) = 26°$, $P(S) = 132°$, and $\Phi_m(S) = 40°$. The molar fraction of the *S*-type conformer varies with temperature from 0.94 (271 K) to 0.79 (346 K).

The influence of solvent condition (D_2O vs $CDCl_3$) on the geometrical parameters as well as on the molar fractions of the *N*- and *S*-type sugar puckers was examined following the same procedure as described in a previous section. It appears that the pseudorotational parameters, *P* and Φ_m, of the α-anomeric sugar conformers are only slightly dependent on solvent condition; the molar fractions X_N and X_S of **1a** are somewhat more dependent on solvent condition ($\Delta X = 0.12$).

Finally, it is found that the conformation of the α-anomeric sugar **3a** incorporated in the tetrameric D oligonucleotide d-(CpSpCpG) (S stands for methyl 2′-deoxy-α-D-ribofuranoside(yl)) is best characterized as a single conformer of the *S*-type: $P(S) = 136°$, $\Phi_m(S) = 39°$.

At this point it is noted that, in view of the accuracy of the observed coupling constants (esd's < 0.2 Hz), the rms values as presented in Table II are rather high, in particular those found for individual analyses of **1a** and **2a** in $CDCl_3$ (0.7 and 0.9 Hz, respectively). Hence, following the guidelines described in a preceding section, the influence of a Barfield correction on the rms deviation between the observed and calculated coupling constants was considered.

In case of the α-anomeric sugar, the Barfield transmission effect is expected to be significant (vide supra) for only one of the two cisoidal coupling constant, i.e. $^3J_{1'2'}$. For example, when a value of 54° for P_b (defining the envelope form $_4E$ is substituted in eq 5, $\Delta^3J_{1'2'}$ yields 1.7 Hz for the *N*-type pucker and 0.1 Hz for the *S*-type pucker. Taking into account the large population of the *S*-type conformer and the relatively small population of the *N*-type conformer, it is obvious that a Barfield correction is of only marginal importance (5%) in relation to the accuracy (rms) of the analysis.

Next, the possibility of pseudolibration[24] of the five-membered ring was examined. In the ^1H NMR pseudorotation analysis described before, the five-membered ring is presupposed to be engaged in an equilibrium between two conformational species. It should be remembered, however, that each species in fact denotes an allowed region of conformations, which is defined by a single continuous potential energy pocket with a minimum at the *P* (Φ_m) value, which has been determined by ^1H NMR. Only when the occupied range occurs over a small (say, $\Delta P = \pm 20°$) pseudorotational region, it is expected (according to test calculations[8]) that pseudolibration of the molecule has a negligible effect on $^3J_{HH}$. In order to obtain some insight into the relative width of the low-energy regions in the potential energy surface of **1a**, MM-2 calculations were carried out. A pseudo-three-dimensional plot of the potential energy (*V*) of **1a** versus *P* and Φ_m is given in Figure 4. The figure shows a single asymmetric energy well with a minimum at $P = 34°$ and $\Phi_m = 40°$. Furthermore, it is noted that the energy well is much broader than the energy pockets calculated for **1b** (not shown). It should be kept in mind, however, that conclusions drawn on the basis of only the contour plot must be considered with caution, because of the low resolution of $V = (P, \Phi_m)$. When full relaxation of **1a** in the MM-2 force field is allowed, starting from the respective structures defined by $P = 0°$ and 180° ($\gamma = 60°$, 180°, and 300°; $\chi' = 60°$), two local minima were found, i.e. at $P(N) = 37°$ ($\Phi_m(N) = 43°$) and $P(S) = 112°$ ($\Phi_m(S) = 41°$).

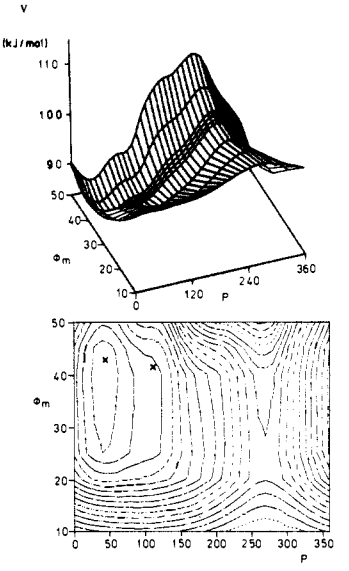

Figure 4. Energy contour plots for **1a**. The maps are contoured to 15.9 kJ/mol from the global minimum at $P = 37°$ and $\Phi_m = 43°$ in increments of 1.3 kJ/mol. The local minima found after free relaxation of the molecule are indicated on the plot by means of crosses.

The MM-2 results are summarized in Figure 3 (track αII). It is shown that the results of both methods, ^1H NMR (track αI) and MM-2, are in excellent agreement *as far as the pseudorotational parameters P(S), $\Phi_m(S)$, and P(N) of the stable minima is concerned*; the *N*-type conformation (MM-2) appears to be more

Table III. Vicinal Coupling Constant Data and Relative Populations X (Molar Fractions) of Gauche$^+$ (g^+), Trans (t), and Gauche$^-$ (g^-) Rotamers about the C_4–$C_{5'}$ Bond of **1a**, **2a**, **3a**, **1b**, and **2b**[a]

	solvent	temp, K	$J_{4'5'}$	$J_{4'5''}$	X_{g^+}	X_t	X_{g^-}
1a	D_2O	271	3.7	4.8	0.51	0.34	0.15
		292	3.7	5.2	0.47	0.38	0.15
		346	3.9	5.4	0.43	0.40	0.17
	$CDCl_3$	292	4.2	4.6	0.49	0.30	0.21
2a	$CDCl_3$	292	3.7	4.2	0.57	0.27	0.16
3a	D_2O	300	2.8	4.2	0.67	0.29	0.04
1b	D_2O	271	4.6	7.3	0.25	0.50	0.25
		292	4.6	7.0	0.28	0.47	0.25
		346	4.9	6.9	0.27	0.43	0.30
1b	$CDCl_3$	292	4.2	5.0	0.51	0.27	0.22
2b	$CDCl_3$	292	6.0	7.0	0.20	0.36	0.44

[a] Molar fractions were calculated following the procedure described in Methods. Calculations were based on the torsion angles of the individual rotamers as denoted before (see text).

puckered ($\Phi_m(N) = 43°$) in comparison with the corresponding structure determined by ^1H NMR ($\Phi_m(N) = 26°$). For the sake of completeness it is noted that the latter discrepancy is to be taken less serious than it seems: it has been shown before[27] that especially Φ_m of a "minor" conformational species is less well determined from a pseudorotational analysis of NMR coupling constants.

As was found for **1b**, the potential energy of **1a** reaches maxima around $P = 90°$ and $P = 270°$. However, the height of the energy barrier at $P = 90°$, calculated for **1a**, appears to be small (2.9 kJ/mol; the energy at $P = 34°$ is taken as the zero point) compared with the corresponding barrier of **1b** (7.5 kJ/mol). Thus, although the structures predicted by MM-2 are in line with the structures indicated by ^1H NMR, we cannot exclude for the time being that a pseudolibrational model for **1a** (spanning a range of e.g. $10° < P < 140°$) would be more satisfactory than the two-state model, which was proposed above.

Conformation of the Exocyclic 5'-CH_2OH. On basis of the $^3J_{4'5'}$ and $^3J_{4'5''}$ coupling constants, an estimate was made of the X_{g^+}, X_t, and X_{g^-} rotamer populations about the C_4–$C_{5'}$ bond (see Methods). It is shown in Table III that the g^+ and t rotamer populations are favored relative to the g^- population. The dominance of the g^+ and t rotamers about C_4–$C_{5'}$, in which the $O_{5'}$-substituent is gauche to the $O_{4'}$-substituent, can be rationalized by assuming a predominant gauche effect, i.e. a strong preference for a gauche O–C–C–O orientation relative to a trans conformation of the corresponding fragment.[28,29] A temperature increase from 271 to 346 K in **1a** (D_2O) is accompanied by a slight decrease in X_{g^+} population ($\Delta X_{g^+} = -0.08$) and increase in X_t population ($\Delta X_t = 0.06$). In contrast, the rotamer distribution of **1b** in D_2O appears to be rather insensitive to temperature (see Table III). As has been discussed already (vide supra), also the N/S equilibrium of **1a** in D_2O is slightly dependent on temperature, whereas that of **1b** in D_2O appears to be virtually independent of temperature.

For ribo- and 2'-deoxyribonucleosides,[30,31] arabinonucleosides,[32] α-ribo- and 2'-deoxy-α-ribonucleoside constituents,[33] a linear relationship between the molar fraction of the N-type sugar conformation X_N and the g^+ rotamer of the exocyclic CH_2OH group has been observed. Moreover, it was found that the g^+ rotamer in the N-type conformation of the nucleoside derivatives mentioned before is at least unfavored (or even forbidden). A similar conformational relation is found for **1a** (D_2O) and **1b** (D_2O), where X_{g^+} appears to vary linearly with X_N (see Table III and Figure 5). Figure 5 shows that the extrapolation of X_{g^+} versus X_N to $X_N = 1$ yielded $X_{g^+} = 0$, which indicates that in the N-type sugar conformation the g^+ rotamer is forbidden in α- and β-glycofuranosides.

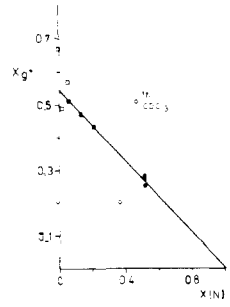

Figure 5. Plot of the molar fraction X_{g^+} of the exocyclic C_4–$C_{5'}$ rotamer versus the molar fraction N-type sugar pucker: for **1a** (filled squares) and **1b** (filled circles) in D_2O; for **1a** ($CDCl_3$), **2a** ($CDCl_3$), **3a** (D_2O) (open squares) and **1b**, **2b** (open circles) in $CDCl_3$.

Further inspection of Figure 5 reveals that the X_{g^+} values of **2a**, **3a**, **1b** ($CDCl_3$), and **2b** deviate substantially from the observed linear relationship. The deviations observed for **2a** and **2b** can be explained by possible sterical interactions of the bulky substituents on the exocyclic groups. In case of **1b** dissolved in $CDCl_3$, the higher value of the molar fraction of X_{g^+} can be explained in terms of an intramolecular hydrogen bond between the $O_{1'}$ acceptor and the 5'-CH_2OH donor, which will stabilize the g^+ conformation. For **3a**, a clear preference for the g^+ rotamer is observed. We note that the latter preference is entirely in accordance with the strong preference for the γ^+ conformation commonly observed[34] in single- and double-helical fragments.

Discussion and Conclusions

A consistent model of the conformational behavior of **1b** is obtained from crystallographic, ^1H NMR, and MM-2 studies. The results of ^1H NMR show that compound **1b** is engaged in a rapid equilibrium between two conformations, i.e. an N- and S-type conformer. The geometry of the N-type conformer can be described as an intermediate conformation between ^1_2T and $_2E$, whereas that of the S-type conformer can be characterized as a ^4E conformation (see Figure 3, track βI). The pseudorotational parameters for both conformers are $P(N) = 335°$, $\Phi_m(N) = 45°$, $P(S) = 234°$, and $\Phi_m(S) = 42°$.

Previously, Gerlt and Youngblood[10] reported a qualitative analysis of the vicinal proton–proton coupling constants of **1b** in D_2O solution on the basis of the method of Davies and Danyluk.[35] Their reported coupling constants, of which the reliability was questioned recently,[11] appear to agree well with the values listed in Table I. However, the authors were not able to interpret their results in a consistent way. Nevertheless, they concluded that the preferred ring conformation is described by a 3'-endo pucker ($P = 18°$). Neither the geometry nor the molar fractions of the N- and S-type conformers found in the present study agrees with those reported by Gerlt and Youngblood.

A very recent paper[11] examined the conformational freedom of **1b** by means of the so-called consistent force field (CFF) method. Although these CFF calculations seem to yield similar conformations for **1b** as found in our MM-2 calculations, we have doubts about the validity of the results reported by Wiórkiewicz-Kuczera and Rabczenko:[11] In their calculations the latter authors assume (without any verification) the exocyclic χ' angle to adopt a trans conformation ($\chi' = 180°$); however, our MM-2 calculations indicate (vide supra) that the steric energy

(27) Haasnoot, C. A. G.; de Leeuw, F. A. A. M.; de Leeuw, H. P. M.; Altona, C. *Biopolymers* **1981**, *20*, 1211.
(28) Wolfe, S. *Acc. Chem. Res.* **1972**, *5*, 102.
(29) Fuchs, B.; Ellencweig, A. *J. Org. Chem.* **1979**, *44*, 2274.
(30) Hruska, F. E. *Proceedings of the International Symposium on the Conformation of Biological Molecules and Polymers*, Symposia on Quantum Chemistry and Biochemistry; Bergmann, E. D., Pullman, B., Eds.; Academic: Jerusalem, 1973; Vol. 5, p 345.
(31) Davies, D. B. In *Nuclear Magnetic Resonance Spectroscopy in Molecular Biology*; Pullman, B., Ed.; Reidel: Dordrecht, The Netherlands, 1978; p 71.
(32) Ekiel, I.; Remin, M.; Darzynkiewicz, E.; Shugar, D. *Biochim. Biophys. Acta* **1976**, *435*, 405.
(33) Cadet, J.; Taieb, C.; Remin, M.; Niemczura, W. P.; Hruska, F. E. *Biochim. Biophys. Acta* **1980**, *608*, 435.
(34) Raap, J.; Dreef, C. E.; van der Marel, G. A.; van Boom, J. H.; Hilbers, C. W. *J. Biomol. Struct. Dyn.* **1987**, *5*, 219.
(35) Davies, D. B.; Danyluk, S. S. *Biochemistry* **1974**, *13*, 4417.

Table IV. Chemical Shift Data (ppm) of **1a**, **2a**, **3a**, **1b**, and **2b**

proton	**1a** (D_2O, 292 K)[a]	**1a** ($CDCl_3$, 292 K)	**2a** ($CDCl_3$, 292 K)	**3a** (D_2O, 300 K)	**1b** (D_2O, 292 K)[a]	**1b** ($CDCl_3$, 292 K)	**2b** ($CDCl_3$, 292 K)
$H_{1'}$	5.161	5.078	5.219	6.188	5.206	5.124	5.276
$H_{2'}$	2.327	2.191	2.541	2.310	2.226	2.238	2.622
$H_{2''}$	1.902	1.967	2.272	2.034	2.159	2.103	2.450
$H_{3'}$	4.245	4.168	5.458	4.610	4.332	4.460	5.666
$H_{4'}$	4.066	4.067	4.548	4.348	3.969	4.019	4.556
$H_{5'}$	3.704	3.667	4.688	4.015	3.690	3.701	4.675
$H_{5''}$	3.620	3.632	4.582	3.941	3.569	3.665	4.537
H_1 (OCH_3)	3.371	3.382	3.443	3.370	3.371	3.361	3.379
H aromatic (center of m)			8.259				8.243

[a] Chemical shift values are independent of temperature, within experimental error, in the range of 271–346 K.

of **1b** increases by ~13 kJ/mol upon changing the χ' value from 300° to 180°. Moreover, examination of four crystal structures of β-glycofuranosides shows that the conformation about the torsion angle χ' is gauche$^-$.[12] Hence, we conclude that the favored conformation about the exocyclic C_1–$O_{1'}$ bond is gauche$^-$,[12] and therefore,[11] the reported "stable" sugar conformations are in fact high-energy conformations and cannot be trusted to give a good description of the conformation of **1b**. Furthermore, the investigators pointed out[11] that calculated values of $^3J_{HH}$ averaged over "appropriate" sets of conformers are in satisfactory agreement with ^{1}H NMR coupling constants of **1b** measured in aqueous solution.[10] However, the rms deviation between the calculated and measured coupling constants is unacceptably large (2.1 Hz), again indicating a serious error in the model used.

As was shown previously for nucleoside constituents,[14,17,26] a statistical analysis of a large body of X-ray structures is informative for the understanding of the conformational features of structural closely related compounds. Until now only a few X-ray structures have been reported for glycofuranosides, of which most belong to the class of ribofuranosides. Nevertheless, their pseudorotational phase angles (P = 301°–356°),[12] which fall clearly outside the range usually observed for the N-type conformations of β-nucleosides,[17] show the same trend as the pseudorotational parameters determined for **1b** by means of ^{1}H NMR and MM-2 (Figure 3).

The results obtained from X-ray crystallography, ^{1}H-NMR, and MM-2 outlined here for α- and β-ribofuranoside derivatives not only establish their characteristic geometrical parameters but also suggest a structural rationale behind the observed pseudorotational behavior of glycofuranosides. In a previous study[12] of the variability of C_1–$O_{1'}$ bond lengths in crystal structures of glycofuranosides, it was shown that the observed pseudorotational phase angle of the sugar ring might reflect the influence of the anomeric effect. Here, we propose that the phase angles of the two different species, which exist in the conformational equilibrium of **1b**, might be indicative that both the anomeric and the gauche effect (vide supra) are operative.

The (endo) anomeric effect and the gauche effect can be monitored by the values of the torsion angles $C_{4'}$–$O_{4'}$–$C_{1'}$–$O_{1'}$ (Φ_3) and $O_{3'}$–$C_{3'}$–$C_{4'}$–$O_{4'}$ (Φ_1), respectively. Both angles are intimately related to the pseudorotational phase angle by eq 6.[18] The

$$\Phi_j = t_j + u_j\Phi_m \cos(P + \epsilon_j + 144j) \qquad j = 1\text{–}4 \qquad (6)$$

parameters t_j, u_j, and ϵ_j of eq 6 were determined from MM-2-calculated structures. The plot of the exocyclic torsion angles of **1b** versus P is shown in Figure 6. The anomeric and gauche effects are expected[36] to be operative in the ranges denoted in the figure by broken lines. The finding of a N-type conformer ($P(N)$ = 335°) can thus be explained by anomeric stabilization of the sugar ring. In contrast the S-type conformer ($P(S)$ = 234°) is stabilized by a predominant gauche effect. It is also shown in Figure 6 that the gauche$^-$ and anomeric effects in **1b** are superimposed at P = 250°, but apparently the intrinsic pseudorotation barrier in the pseudorotation circuit around P = 270° supersedes

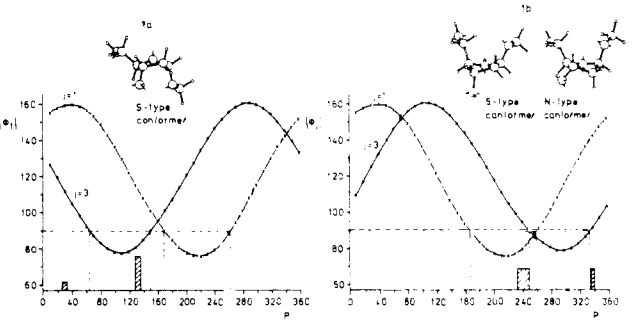

Figure 6. Plot of two exocyclic torsion angles ($C_{4'}$–$O_{4'}$–$C_{1'}$–$O_{1'}$) (j = 3 in eq 6) and ($O_{3'}$–$C_{3'}$–$C_{4'}$–$O_{4'}$) (j = 1 in eq 6) versus the pseudorotational phase angle P for **1b** and for **1a** (Φ_m = 40.0°). Phase angles of experimentally (^{1}H NMR) observed conformers are indicated by hatched bars. The height of each bar is proportional to the molar fraction of the specific conformer.

this favorable effect.[25,26,37]

In addition, a consistent model for the conformational features of **1a** is obtained from ^{1}H NMR and molecular mechanics following the same line of reasoning. The strong preference of the S conformer ($P(S)$ = 132°, $\Phi_m(S)$ = 40°) over the N conformer ($P(N)$ = 29°, $\Phi_m(N)$ = 26°) can again be rationalized qualitatively in terms of gauche and anomeric effects. In this case, however, the stabilization of the S-type conformer is attributed to superimposed anomeric and gauche effects (Figure 6).

Our observations for 2′-deoxy-α-D-ribofuranosides and 2′-deoxy-β-D-ribofuranosides lead to the conclusion that both the oxygen at position 1′ (anomeric effect) and the oxygen at position 3′ (gauche effect with respect to $O_{4'}$) are of major importance for determining the conformational features of the base-deleted sugar. Hence, **1a** and **1b** will simulate the conformational properties of 2′-deoxy-D-ribofuranose better than the sugar derivatives 1′,2′-dideoxy-D-ribofuranose and 1′-(2′-deoxy-β-D-ribofuranosyl) cyanide, which were used in conformational studies of base-deleted oligonucleotides reported so far.[4,9] At this point one speculates about a crucial step in the repairing process of a base deletion in the DNA molecule: the recognition of the AP site by repairing proteins. Assuming that this recognition depends, among other factors, on conformational differences between 2′-deoxy-α-ribofuranosyl and 2′-deoxy-β-ribofuranosyl residues on the one hand and the four building blocks of DNA (dC, dG, dT, and dA), on the other hand, we have presented evidence that the conformational behavior of 2′-deoxy-α-D-ribofuranose is similar to that of 2′-deoxynucleosides, whereas, in contrast, the conformational characteristics of 2′-deoxy-β-D-ribofuranose differ significantly from those of the nucleic acid constituents. Therefore, it might be speculated that the conformational behavior of the β form of an AP site in DNA is a more important factor in the recognition process than that of the α form.

Experimental Section

^{1}H NMR measurements of the nonexchangeable protons were carried out in 99.95% D_2O in which the samples were dissolved after threefold

(36) Smits, G. F. Ph.D. Thesis, University of Leiden, The Netherlands, 1985.

(37) Levitt, M.; Warshell, A. *J. Am. Chem. Soc.* **1978**, *100*, 2607.

lyophilization from 99.8% D_2O. Proton NMR spectra were recorded on a Bruker WM-300 spectrometer. Suppression of the residual HDO peak was achieved by a low-power selective irradiation pulse (during 0.8 s).

The assignments of the resonances in the spectra (Tables III and IV) to individual protons are based on the following rationales: The H_1 (OCH_3) resonance is readily recognized as a singlet at 3.4 ppm. Vicinally coupled pairs of protons were identified by extensive decoupling experiments. The stereochemical assignment of the geminal $H_{2'}$ and $H_{2''}$ is based on coupling constant considerations. The assignments of the $H_{5'}$ and $H_{5''}$ signals conform to the assignment reported previously for tetrahydrofuranmethanol.[10] The resolution-enhanced 300-MHz spectra were computer simulated with a LAOCOON-type computer program of which the standard plot routines were extended[38] in order to reproduce Gaussian line shapes with negative side lobes.

Pseudorotational phase angles (P), puckering amplitudes (Φ_m), and mole fractions of conformers (X_N, X_S) were calculated from the experimental vicinal coupling constants with the computer program PSEUROT. This program is based on algorithms as described by Haasnoot et al.[8] and De Leeuw et al.[39,40]

Acknowledgment. This research was supported by The Netherlands Foundation for Chemical Research (SON) with financial aid from The Netherlands Organization for the Advancement of Pure Research (ZWO). We gratefully acknowledge the stimulating discussions with Prof. Dr. C. W. Hilbers and Prof. Dr. C. Altona.

(38) Mellema, J.-R.; Pieters, J. M. L.; van der Marel, G. A.; van Boom, J. H.; Haasnoot, C. A. G.; Altona, C. *Eur. J. Biochem.* **1984**, *143*, 285.

(39) de Leeuw, F. A. A. M.; Altona, C. *J. Comput. Chem.* **1983**, *4*, 438.
(40) de Leeuw, F. A. A. M.; Altona, C. *QCPE* **1983**, *463*.

Aqueous Coordination and Location of Exchangeable Cu^{2+} Cations in Montmorillonite Clay Studied by Electron Spin Resonance and Electron Spin-Echo Modulation

David R. Brown[†] and Larry Kevan*

Contribution from the Department of Chemistry, University of Houston, Houston, Texas 77004.
Received June 23, 1987

Abstract: Electron spin resonance (ESR) and electron spin-echo modulation (ESEM) spectroscopies have been used to characterize the aqueous coordination and location of exchangeable Cu^{2+} cations in the interlayer regions of montmorillonite clay. Mg^{2+} montmorillonite, in which 5% of the exchangeable cations were replaced by Cu^{2+}, was investigated. Under complete hydration, ESR indicates freely rotating Cu^{2+} ions in the interlayer region, and the corresponding ESEM indicates six directly bound water molecules. Under partial dehydration ESR shows Cu^{2+} in a second site with restricted rotation, and the corresponding ESEM indicates coordination to four water molecules. Following the collapse of the aqueous interlayer region on further dehydration, the Cu^{2+} enters a third site in a hexagonal cavity of the lattice structure, also with restricted rotation, in which it remains coordinated to only one water molecule. The natures and interconversions of these three sites are discussed.

The two swelling phyllosilicates, montmorillonite and hectorite, are members of the smectite group of clays. These clays have a layered structure in which rigid layers of silicate ions are separated by aqueous interlayer regions containing hydrated cations as shown in Figure 1. The thickness of the aqueous interlayer region is sensitive to ambient conditions and can readily be varied from many molecular layers to almost zero by controlled hydration and dehydration. The location and solvation of the cations in this interlayer region depend on several factors, including the thickness of the aqueous interlayer, the location and abundance of anionic sites in the clay lattice, and the presence of cavities in the clay lattice which can accomodate and chelate the cations.

The anionic lattice sites in montmorillonite and hectorite are in the middle, octahedral, layer of the smectite structure, and as such they are separated from the cations by the upper and lower tetrahedral layers. The relatively weak electrostatic attraction between cations and anionic sites means that, under appropriate conditions, the cations can move away from the silicate surface into the body of a strongly solvating solvent, where strong solvation compensates for the increased electrostatic potential energy. On removal of the solvent by dehydration cations are thought to enter hexagonal cavities in the silicate lattice.[1] These have internal diameters of about 0.5 nm and can accomodate all but the largest cations. Once in these cavities cations are coordinated by lattice oxygens.

Several techniques have been used to study cation locations in clays. X-ray diffraction has been of limited use because of the poor crystallinity typically exhibited by clays. Among other spectroscopic techniques electron spin resonance (ESR) has been one of the most successful, even though its use is limited to clays containing paramagnetic centers.[2-5]

An ESR study of a magnesium hectorite, in which 5% of the exchangeable cations were replaced with Cu^{2+}, revealed two discrete Cu^{2+} centers, one dominating in fully hydrated clay and a second in clay that has been equilibrated at room temperature and 40% relative humidity.[3] The appearance of these two species was correlated with different d_{001} basal spacings determined from X-ray powder diffraction. The first Cu^{2+} center was assigned to a fully hydrated, freely rotating Cu^{2+} in an aqueous layer of several water molecular thicknesses. The second Cu^{2+} center was associated with a water interlayer of thickness 0.5 nm, and was assigned to a rotationally restricted $[Cu(H_2O)_6]^{2+}$ solvate. However, the aqueous coordination numbers have only been inferred and have not been directly determined.

[†] Present address: Department of Applied Science, Leeds Polytechnic, Leeds, LS1 3HE, England.

(1) Grim, R. E. *Clay Mineralogy*, 2nd ed.; McGraw-Hill: New York, 1968.
(2) Pinnavaia, T. J. In *Advanced Techniques for Clay Mineral Analysis*; Fripiat, J. J., Ed.; Elsevier: New York, 1981; p 139.
(3) McBride, M. B.; Pinnavaia, T. J.; Mortland, M. M. *J. Phys. Chem.* **1975**, *79*, 2430.
(4) Clementz, D. M.; Pinnavaia, T. J.; Mortland, M. M. *J. Phys. Chem.* **1973**, *77*, 196.
(5) McBride, M. B. *Clays Clay Miner.* **1982**, *30*, 200.

0002-7863/88/1510-2743$01.50/0